



EUROfusion

EUROFUSION WPPMI-CP(16) 15752

B Koncar et al.

Thermal radiation analysis of DEMO tokamak

Preprint of Paper to be submitted for publication in
Proceedings of 29th Symposium on Fusion Technology (SOFT
2016)



This work has been carried out within the framework of the EUROfusion Consortium and has received funding from the Euratom research and training programme 2014-2018 under grant agreement No 633053. The views and opinions expressed herein do not necessarily reflect those of the European Commission.

This document is intended for publication in the open literature. It is made available on the clear understanding that it may not be further circulated and extracts or references may not be published prior to publication of the original when applicable, or without the consent of the Publications Officer, EUROfusion Programme Management Unit, Culham Science Centre, Abingdon, Oxon, OX14 3DB, UK or e-mail Publications.Officer@euro-fusion.org

Enquiries about Copyright and reproduction should be addressed to the Publications Officer, EUROfusion Programme Management Unit, Culham Science Centre, Abingdon, Oxon, OX14 3DB, UK or e-mail Publications.Officer@euro-fusion.org

The contents of this preprint and all other EUROfusion Preprints, Reports and Conference Papers are available to view online free at <http://www.euro-fusionscipub.org>. This site has full search facilities and e-mail alert options. In the JET specific papers the diagrams contained within the PDFs on this site are hyperlinked

Thermal radiation analysis of DEMO tokamak

Boštjan Končar^a, Martin Draksler^a, Oriol Costa Garrido^a, Botond Meszaros^b

^aJožef Stefan Institute, Reactor Engineering Division

^bPPPT, PMU, Eurofusion

Thermal radiation analysis of the DEMO tokamak based on the 2015 baseline CAD design model was performed. For the purpose of analysis, Vacuum Vessel Thermal Shield (VVTS) and Cryostat Thermal Shield (CTS) were designed on a conceptual level to complement the baseline DEMO CAD model. The Finite Element (FE) code ABAQUS was used to perform numerical analyses. A special care was taken to adapt the geometry and mesh of the FE model to reduce the heat transfer error to an acceptable level. Thermal loading on DEMO components and refrigeration power for the base case scenario with actively cooled thermal shields was determined. Besides the base case, the sensitivity analysis with passive CTS was performed.

Keywords: thermal radiation analysis, DEMO tokamak, Finite Element modeling.

1. Introduction

The demonstration fusion power plant DEMO [1] will be last major step between ITER and a commercial fusion power plant and will have to demonstrate the stable long term operation with the net electricity production of few hundred MWs. To support the development of a consistent design, a global thermal radiation analysis of the DEMO tokamak has been performed by the Jožef Stefan Institute (JSI) within the EUROfusion project [2]. The objective of the analysis is to evaluate the radiative heat exchange between tokamak components operating at different temperatures and to predict the thermal loadings on individual components.

Thermal model is based on the recent baseline CAD design of main tokamak components [3]. For the purpose of analysis, Vacuum Vessel Thermal Shield (VVTS), and Cryostat Thermal Shield (CTS) were designed on a conceptual level [2] to complement the baseline DEMO CAD model. The Finite Element (FE) code ABAQUS [4] was used to perform numerical analyses. Thermal radiation simulations in complex geometries can be largely affected by numerical errors due to calculation of geometrical view factors. Hence a special care was taken to adapt the geometry and mesh of the FE model to reduce the heat transfer error to an acceptable level. The main simulation results provide thermal loading on different DEMO systems and components and enable the calculation of minimum refrigeration power required to cool the magnet systems and thermal shields. In addition, the possibility of having a fully passive CTS was investigated. Besides the base case with actively cooled thermal shields, two configurations with passive CTS were also analyzed.

2. DEMO thermal radiation model

Thermal model of DEMO tokamak is composed of several systems operating at different temperatures under vacuum conditions. Thermal radiation is assumed to be the prevailing heat transfer mechanism. In a global heat transfer analysis of DEMO tokamak direct heating of in-vessel components by escaped plasma particles and

internal heating due to neutron irradiation are not modeled explicitly. The deposited heat in the divertor, blanket and vacuum vessel is removed by active coolant systems, assuming that they keep the components at constant temperatures. Low temperature components outside the vacuum vessel – superconducting magnets and thermal shields are also actively cooled, while the cryostat containment is assumed to be at room temperature.

DEMO tokamak FE model is shown in Fig. 1. Major components considered in the thermal analysis are as follows: CRY (Cryostat), CTS, magnet system including six PFC (Poloidal Field Coils), TFC (Toroidal Field Coils) and central solenoid (SOLENOID), VVTS, VV (Vacuum Vessel with 4 ports), BLA (Blanket) and DIV (Divertor). All four VV ports are closed by lids to ensure completely closed geometry of the tokamak.

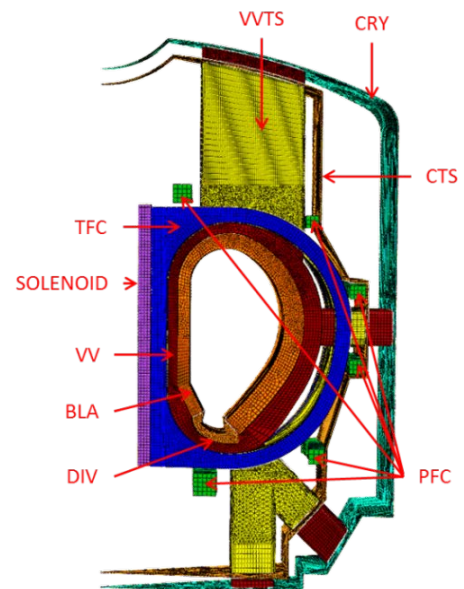


Fig. 1. Global DEMO tokamak model.

Taking into account the symmetry in toroidal direction, thermal radiation heat exchange between the components is calculated for the 20° section (1/18th) of

the tokamak [2]. Emissivities, materials and temperatures of the components during operating conditions are listed in Table 1 and were defined in task specifications of the project [5]. Note that the emissivity of the magnets is conservatively set to the value of 1.

Table 1: DEMO normal operation conditions.

Component	T (K)	ε	Material
BLA, DIV	573	0.25	F82H-Eurofer
VV	473	0.25	SS-316
Magnets	4	1	SS-316
CTS, VVTS	80	0.05	SS-304
CRY	293	0.25	SS-304

3. Numerical solution

Numerical simulations were performed with the FE solver code ABAQUS [4]. The radiation heat exchange in the tokamak is modeled as a closed cavity thermal radiation problem [6]. The exchange of radiation between the opposing surfaces strongly depends on their geometry, orientation, as well as on their radiative properties and temperatures. Each surface is composed of small elemental surfaces, termed as facets. In the cavity radiation formulation [4], the radiation heat flux q_i [W/m²], into a cavity facet is defined as

$$q_i = \sigma \varepsilon_i \sum_{j=1}^N \varepsilon_j \sum_{k=1}^N F_{ij} C_{ji}^{-1} (T_j^4 - T_i^4), \quad (1)$$

where N represents the number of facets forming the cavity, ε_i and T_i represent the emissivity and the temperature of the facet i , $\sigma=5.67 \times 10^{-8}$ W/m²K⁴ is the Stefan-Boltzmann constant, F_{ij} is the geometrical view factor matrix and $C_{ji} = \delta_{ij} - (1 - \varepsilon_i)F_{ij}$ is the reflection matrix with δ_{ij} denoting Kronecker delta function. Numerically, the radiation heat exchange between two arbitrary facets is defined by the concept of view factors [6] schematically presented in Fig. 2.

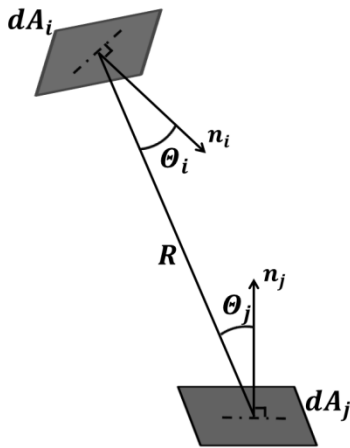


Fig. 2. Schematic representation of the view factor between the facets dA_i and dA_j separated by a distance R .

The view factor F_{ij} is defined as the fraction of the radiation leaving the facet dA_i that is intercepted by the facet dA_j [6]:

$$F_{ij} = \frac{1}{A_i} \int_{A_i} \int_{A_j} \frac{\cos \theta_i \cos \theta_j}{\pi R^2} dA_i dA_j, \quad (2)$$

where R is the distance between the surfaces i and j , θ_i and θ_j are polar angles between R and normals to surfaces. For closed cavity problem, the view factor calculation also satisfies reciprocity ($A_i F_{ij} = A_j F_{ji}$) and summation relation ($\sum_{j=1}^N F_{ij} = 1$) [6]. Ideally, the total radiation heat exchange between all systems in a closed cavity simulation should be equal to zero ($\sum Q_i = 0$), where Q_i denotes the net radiation heat flow for the i -th surface (difference between the received and emitted radiative heat flow in Watts).

However, in numerical simulations the energy balance is never completely preserved, mainly due to numerical errors arising from spuriously calculated view factors. The relative error of the simulation is defined as the ratio between the sum of all net radiative heat flows in the tokamak and the average of all absorbed and emitted heat flows (absolute values) exchanged in the tokamak system:

$$Relative\ error = \frac{\sum_i Q_i}{(\sum_i |Q_i|)/2}. \quad (3)$$

3.1 Grid refinement and error reduction

Meshing turned out to be the most important step in the model development having the strongest impact on the simulation error. The number of facets with erroneous view factors can be substantially reduced if the mesh topology is adapted to the model geometry. Therefore, all sharp edges of opposite facing components are projected to the surfaces which are being meshed. In this case, the facet cannot interact with both accompanying surfaces next to the sharp edge, which has been identified as one of the reasons for the inaccurate calculation of view factor. For example, all sharp edges of the magnet systems were projected to VVTS outer surface as shown in Fig. 3.

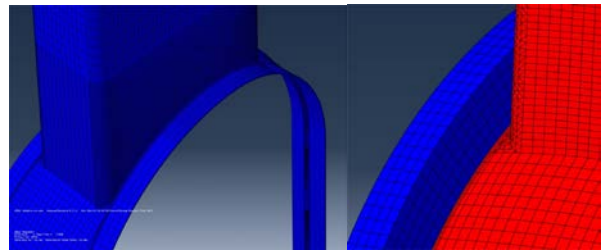


Fig. 3: Vacuum vessel thermal shield with detailed mesh (left). TFC in close proximity of the VVTS (right).

4. Results

The simulation results for the base case configuration where both thermal shields (VVTS, CTS) are actively-cooled are presented in Table 2. The net radiation heat flows (in kW) on the components for the complete tokamak geometry are given in the second column. The positive net heat flow indicates that the component absorbs radiation from its surrounding, while the

negative values indicate that the component is a net emitter. As expected, hot in-vessel components (BLA, DIV) and VV are net emitters whereas the cooler components (outside VV) are net absorbers. The highest heat flow is absorbed by the VVTS since it encloses the entire VV. The cryostat also absorbs a substantial amount of radiative heat flow since it interacts with VV ports. On the other side, the absorbed heat flow in the magnets is rather low (1.26 kW) since these components are being shielded from all sides by actively cooled VVTS and CTS at 80 K. Corresponding heat fluxes (in W/m^2) distinguishing between the emitted and absorbed heat loads for specific component are also presented in Table 2. For example VV with ports absorbs $123 W/m^2$ of radiative heat flux from the blankets and divertor, while it emits about $181 W/m^2$ to the VVTS. VV with ports is therefore the net emitter ($-58.2 W/m^2$).

Heat loads from the thermal shields and magnet systems have to be removed through the refrigeration process using the cryoplant. In the base case thermal shields are assumed to be cooled by helium at 80 K and the cooling of super-conducting magnets is supposed to be realized by the liquid helium keeping the magnets at 4 K. According to Carnot principle, in the ideal case, refrigeration requires minimum specific power to extract a given heat from a desired cooling temperature to a heat sink at ambient temperature T_{amb} . The minimum specific refrigeration power P_i^{refrig} required to keep the actively-cooled component i at the temperature T_i is calculated as follows [7]:

$$P_i^{refrig} = q_{i,net} \left(\frac{T_{amb} - T_i}{T_i} \right), \quad (4)$$

where $q_{i,net}$ is the net heat flux on the i -th component. The total specific refrigeration power of a system, ($P_{tot} = \sum P_i$) is defined as the sum of individual powers for VVTS, magnets and CTS, Based on the simulation

results, the total refrigeration power per unit area for both shields and magnets amounts to $430 W/m^2$.

All heat flux values presented in Table 2 are averaged across the surfaces of the component. Due to the geometry of the components the radiative heat load can be rather unevenly distributed. As an example, simulated radiation heat flux distribution on the magnets is shown in Fig. 4. It can be seen that the upper surface of the PFC and TFC close to the upper port receive the highest radiation heat load as a result of the geometry of the VVTS and CTS in this region (more of the thermal shield surface is visible to magnets). Though still low, the peak heat flux on the second poloidal field coil ($\sim 0.8 W/m^2$) is about four times higher than the averaged heat load ($\sim 0.2 W/m^2$) on the entire magnet system.

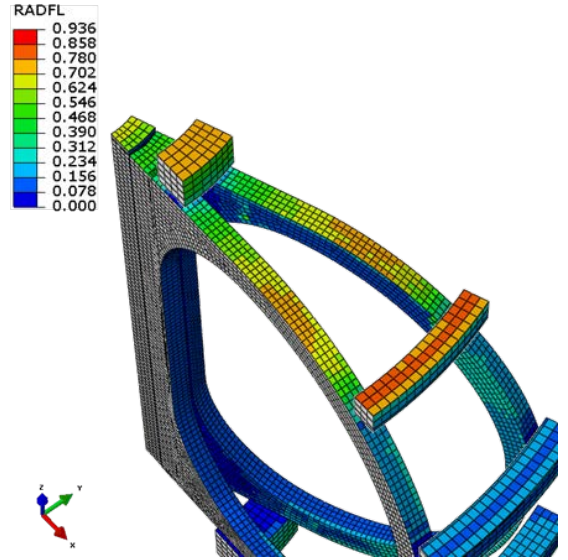


Fig. 4: Heat flux distribution on the magnets.

Table 2: Base case scenario with thermal shields actively cooled at 80 K – complete DEMO tokamak

Component	$(Q_{i,net})$ Net Heat Flow (kW)	(q_i) Heat Flux (W/m^2)			P_i^{refrig} (W/m^2)
		Emitted	Received	Net	
BLA	-916.38	-271.5	-	-271.5	-
DIV	-119.16	-244.3	-	-244.3	-
VV with ports	-495.8	-181.4	123.2	-58.2	-
VVTS	893.36	-0.09	121.1	121.0	322.3
Magnets	1.26	-	0.19	0.19	13.0
CTS	148.47	-0.09	35.4	35.3	93.9
CRY	416.52	-	7.5	75.5	-
TOTAL	-71.74	Relative error -4.8%			429.2

4.1 Sensitivity analysis with passive CTS

To avoid active cooling of the CTS, the possibility of having a fully passive CTS was investigated. Two sensitivity cases were performed. In CASE 1, CTS is assumed to be fully passive (without cooling), while in the CASE 2, one Multi-Layer Insulation (MLI) package

is added between the fully passive CTS and the Cryostat. The CTS is modeled as a 3 mm thick shell with a thermal conductivity of $16.2 W/mK$ [8]. MLI characteristics used for the CASE2 are taken from the W7-X data [9], where one MLI package with the thickness of 15 mm consists of 20 layers and has a thermal conductivity of $0.1 W/mK$ [9] and the same

emissivity as CTS (see Table 1). The heat loads for the cases with passive CTS are presented in Table 3.

Table 3: Cases with passive CTS - complete DEMO tokamak

Component	Net Heat Flow (kW)	Heat Flux (W/m^2)	P_i^{refrig} (W/m^2)
CASE1 – passive CTS			
VVTS	903.6	121.8	324.3
Magnets	63	9.6	690.7
CTS	0	0.0	-
Total			1015
CASE2 – passive CTS with MLI			
VVTS	898.2	121.1	322.6
Magnets	32.4	4.7	358.4
CTS	0	-	-
MLI	0	-	-
Total			681.0

For passive CTS (CASE1), the absorbed heat from the cryostat is balanced by emitted radiation towards the magnets, amounting to zero net thermal load. The simulated temperature distribution on the passive CTS is shown in Fig. 5. The non-homogeneous temperature distribution ranges between 274 and 312 K with a maximum reached on the parts of CTS surrounding the VV ports. The average temperature of the CTS obtained in the simulation is 289 K.

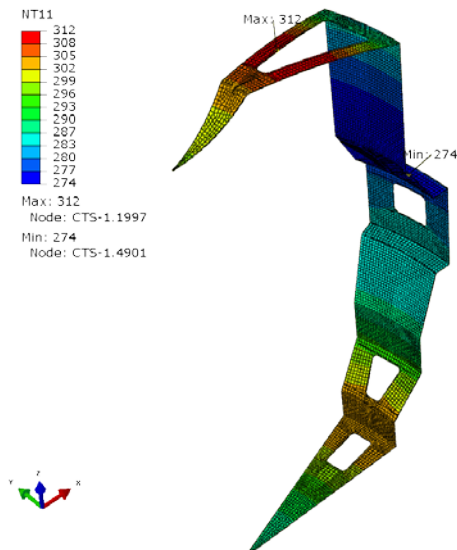


Fig. 5: CASE1: Temperature on the CTS in [K].

Due to the significantly higher CTS temperature comparing to the actively-cooled CTS case (80 K), the thermal load on the magnets is 50 times higher in CASE1 and 25 times higher in the case with additional MLI (CASE2). Thermal loads on other components (DIV, BLA, CRY) remain practically unchanged, hence they are not shown in Table 3.

Increased heat load on the magnets affects also the total refrigeration power. Specific total refrigeration power amounts $1015 W/m^2$ (CASE1) and $681 W/m^2$ (CASE2) and is much higher than in the case of active CTS ($429 W/m^2$).

5. Conclusions

Steady-state thermal radiation exchange between different tokamak systems is analyzed numerically with the FE code ABAQUS. In order to reduce the energy imbalance in simulation, extensive grid refinement study has been performed. The final energy imbalance for the full tokamak model was reduced below 5%. For the base case configuration with actively cooled VVTS and CTS, the highest heat flow (~900 kW) has to be removed by VVTS, whereas the absorbed heat flow by the magnets is relatively low (~1.2 kW). The simulation results show that localized thermal radiation heat fluxes can be several times higher than the averaged heat flux on the considered component. Detailed 3D numerical analyses are therefore necessary. The minimum specific refrigeration power for cooling of both thermal shields and magnets was determined. The base case, involving only actively cooled components, is characterized by the smallest thermal loading on the magnet system, and the lowest refrigeration power required for component cooling. For comparison, also configurations with passive CTS (CASE1) and with passive CTS including MLI (CASE2) were investigated. By the use of passive CTS (CASE1), the heat load on the magnet system is increased by 50 times resulting in 2.3 times higher total refrigeration power. By adding the MLI on the warm side of the CTS, temperature of CTS and thermal loading on magnets reduce. Nevertheless, still 60% higher refrigeration power is required comparing to the base case.

Acknowledgments

This work has been carried out within the framework of the EUROfusion Consortium and has received funding from the Euratom research and training programme 2014 - 2018 under grant agreement No 633053. The views and opinions expressed herein do not necessarily reflect those of the European Commission.

References

- [1] F. Romanelli, et al., "Fusion Electricity – A roadmap to the realisation of fusion energy", (EFDA), 2012
- [2] B. Končar, M. Drakšler, O. Costa Garrido, I. Vavtar, Thermal analysis of DEMO tokamak 2015, Deliverable PMI-3.2-T03-D01, Jožef Stefan Institute, 2016.
- [3] Baseline CAD Configuration Model: 2D3FBB, May 2015
- [4] ABAQUS 6.13-4, Available: <http://www.simulia.com/>
- [5] B. Mezsáros, Task specifications - Global Tokamak thermal analysis, PMI-3.2-T03, April 2015.
- [6] Incropera, DeWitt, Bergman, Lavine, Fundamentals of Heat and Mass Transfer, United States of America, 2006, pp. 811-878
- [7] M. Wanner, Study of the optimum temperature of the thermal shield of JT-60SA, 2008.
- [8] V. Barabash, Summary of Material Data For Structural Analysis of the ITER Cryostat, 2010.
- [9] M. Nagel, S. Freundt, H. Posselt, Thermal and mechanical analysis of Wendelstein 7-X thermal shield, Fusion Eng. Des. 86 (2011) 1830-1833